Journal of Zhejiang University-SCIENCE A (Applied Physics & Engineering)
ISSN 1673-565X (Print); ISSN 1862-1775 (Online)
www.zju.edu.cn/jzus; www.springerlink.com
E-mail: jzus@zju.edu.cn

Misalignment analysis of journal bearing influenced by asymmetric deflection, based on a simple stepped shaft model*

Zhen-peng HE†1, Jun-hong ZHANG†1, Wei-song XIE†2, Zhou-yu LI[1], Gui-chang ZHANG[1]

([1]*State Key Laboratory of Engine, Tianjin University, Tianjin 300072, China*)

([2]*Deparment of Mathematics, School of Science, Tianjin University, Tianjin 300072, China)*

†E-mail: hezhenpeng@tju.edu.cn; zhangjh@tju.edu.cn; weis_xie@tju.edu.cn

Received Mar. 28, 2012; Revision accepted July 20, 2012; Crosschecked Aug. 17, 2012

Abstract: The effects of journal misalignment on a journal bearing caused by an asymmetric rotor structure are presented in this study. A new model considering the asymmetric deflection is applied. Also, the thermo-hydrodynamic of the oil film in the journal bearing and straightforward elasticity theory are considered in the analysis. Based on the structure stiffness equivalent characteristic, a simple stepped shaft can reflect the entire complex structure model. The existing lubrication model, which does not consider this angle component, is not very precise for journal bearings. Film pressure, misalignment angle, velocity field, oil leakage, and temperature field were calculated and compared in the journal bearing analysis. The results indicate that bearing performances are greatly affected by misalignment caused by the asymmetric structure. A simple stepped shaft can effectively represent a misaligned journal bearing in a rotor-bearing system.

Key words: Misalignment, Stepped shaft, Asymmetric structure, Journal bearing
doi:10.1631/jzus.A1200082 **Document code:** A **CLC number:** TH133.31

1 Introduction

Journal bearings have been widely used in rotor systems. Misalignment exists generally in journal bearings due to the shaft deformation under load, deflection of the shaft, manufacturing errors, assembly errors, improper installation, and asymmetric loads. During operations, misalignment has a considerable effect on the performance of a rotor system, and can even cause wear and vibration to become more serious.

The shaft and journal bearing are usually calculated separately in the design of mechanisms which involve a shaft and journal bearing. The coupled relationship between the shaft and the journal bearing is not considered. In the design of a shaft and bearing, the analysis of shaft stress is usually simplified with the oil film pressure as the concentrative force, and the bearing design does not consider misalignment. In fact, the shaft becomes deformed when subjected to a force, which results in misalignment occurring in the bearing hole and the oil film distribution becoming inclined to one side. However, to satisfy the special function of machines, a shaft is designed to be very complex, and the structure is not symmetrical. Therefore, it is also very important to investigate the effects of misalignment on the lubrication of rotor systems with complex structures.

McKee and McKee (1932) first analyzed the effects of misalignment on pressure distribution in the axial direction of a journal bearing. Dubois *et al*. (1957) experimentally investigated the pressure field and the misalignment of couples under journal misalignment. Smalley and McCallion (1966) analyzed the effect of misalignment on the performance of a full journal bearing under steady state. Pinkus and Bupara (1979) presented a comprehensive analysis of

* Project supported by the National Natural Science Foundation of China (No. 60879002), and the Tianjin Support Plan of China (No. 10ZCKFGX03800)

© Zhejiang University and Springer-Verlag Berlin Heidelberg 2012

misaligned bearings and charts which revealed some of the salient features of different misaligned journal bearings. Buckholz and Lin (1986) analyzed the effect of journal bearing misalignment on load and cavitation for partial arc journal bearings lubricated by non-Newtonian lubricants. Vijayaraghavan (1989) analyzed the effect of cavitation on the performance of a line-grooved misaligned bearing for both flooded and starved inlet conditions. Banwait *et al*. (1998) observed the thermo-hydrodynamic effects in a misaligned circular plain journal bearing. Guha (2000) solved the problem of isotropic steady-state characteristics of hydrodynamic journal bearings considering the isotropic roughness effect. Later, Das *et al.* (2002) used micro-polar fluids to analyze the performance of a misaligned hydrodynamic journal bearing. They also compared the misalignment moment and friction parameters of a journal bearing under different eccentric ratios and misalignment angles. Bouyer and Fillon (2002) experimentally analyzed misalignment effects on performance with a plain journal bearing of 100 mm diameter. Gulwadi and Shrimpling (2003) studied the effect of shaft tilting due to moment acting on it during an engine cycle. El-Butch and Ashour (2005) analyzed the performance of a misaligned tilting-pad journal bearing under transient loading condition. Pierre *et al*. (2002; 2004) compared experimental data and theoretical results of a thermo-hydrodynamic study of a misaligned plain journal bearing. They also studied the thermo-hydrodynamic behavior of misaligned plain journal bearings with theoretical and experimental approaches under steady-state conditions. Sun and Gui (2005a; 2005b) researched the effects of journal misalignment caused by shaft deformation under static and rotary loads on journal bearing lubrication. Later, Sun *et al.* (2010) presented lubrication characteristics under misalignment based on a thermo-hydrodynamic lubrication model. The temperature of the oil film was investigated under different misalignment angles and the roughness of the surface was considered. Jang and Khonsari (2010) took into account film rupture and reformation, and provided a comprehensive analysis of misaligned journal bearings based on a 3D mass-conservative thermo-hydrodynamic model. With the development of the computer technology, the computational fluid dynamics (CFD) is used to gain more precise analysis of the misalignment, for example, Li *et al*. (2012) used the Fluent software to analyze the transient flow of the misaligned journal bearing in the flexible rotor-bearing systems.

The above lubrication analyses of misaligned journal bearings were conducted under some given preconditions or considered a very simple shaft, such as a beam. They did not consider the complex structure characteristics and asymmetrical rotor structure that contributes to the misalignment angle. The analysis of bearings separately will influence the precision of the lubrication design. It is important to make the lubrication analysis more closely represent the actual situation to ensure that it is usable in journal bearing design. In this paper, a numerical analysis model of journal bearing lubrication combined with the rotor structure is developed, and it is solved using the MATLAB program. Therefore, a new misalignment analysis method based on the structure characteristics is applied to the misaligned journal bearing. The advantage of this theory for solving the stepped model is that it is also suitable for other complex rotors. Based on the simplified shaft method, the calculation of misalignment angle in the asymmetric rotor is developed and used to analyze the effects of the structure parameters and the angle caused by asymmetric deflection on the pressure distribution, oil leakage, velocity field, and temperature field of the journal bearing. The results of this work provide a basis for studying the nonlinear dynamic of complex rotor systems and can also provide a theoretical guide for the design of rotor systems.

2 Theory

2.1 Angle of journal misalignment of a simple rotor

The force $2F$ acts on a part of the rotor causing shaft deformation. Hence, the journal misalignment angles γ_1 and γ_2 are found in the two bearing holes, respectively. Deformation of the shaft results from several forces, such as the eccentric force and the transfer force from gear. However, although the exciting forces may be complex, all the forces can be simplified as the concentrative force. Misalignment occurs in the bearing housing. Shaft deformation involving two steps is shown in Fig. 1, where L_1 is the

length of beam AB, L_2 is the length of beam AC, and C is the center of beam BD.

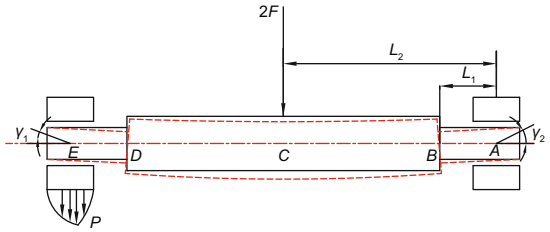

Fig. 1 Misalignment angle of a rotor system under force

Derivation of the misalignment angle of a shaft with two steps can be divided into two processes. Overlay method in elastic theory is used to calculate the deflection and misalignment angles. First, divide the AC beam into AB and BC (Fig. 2). For a symmetrical rotor, the support force of every bearing is equal to F. However, if the exciting load F does not act on the middle of the rotor, the bearing force of every bearing can be calculated by moment balance rules.

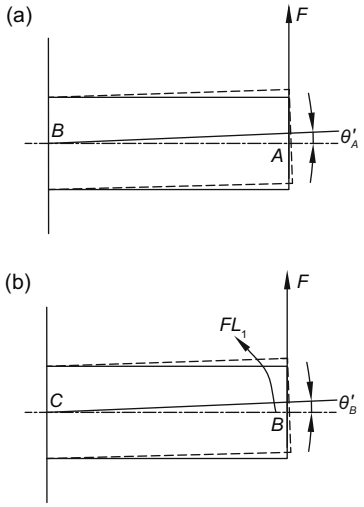

Fig. 2 Overlay method to analyze the misalignment angle
(a) Force model of beam AB; (b) Force model of beam BC

When beam AB is viewed as B side fixed and force F acts on the A side, the deflection and misalignment angles of position A can be expressed as

$$\theta'_A = \frac{FL_1^2}{2EI_1}, \tag{1}$$

$$y'_A = \frac{FL_1^3}{3EI_1}, \tag{2}$$

where $I_1 = \pi(D^4 - d_0^4)/64$, D is the diameter of every step. To save material, the shaft is usually made hollow. The diameter of the hollow space d_0 has a great effect on the section moment of inertia.

When shaft BC is viewed as C side fixed, moment FL_1 exists on the B side, and force F acts on the B side, the deflection and angle of position B can be defined as

$$\theta_B = \frac{F(L_2 - L_1)^2}{2EI_2} + \frac{F(L_2 - L_1)L_1}{EI_2}, \tag{3}$$

$$y_B = \frac{F(L_2 - L_1)^3}{3EI_2} + \frac{F(L_2 - L_1)^2 L_1}{2EI_2}. \tag{4}$$

According to the material's properties, the deflection curve is a continuous smooth curve, and the deflections and angles of shafts AB and BC are the same at position B. When the shaft BC deforms, the shaft AB keeps straight but must rotate by angle θ_B. It contributes another deflection y''_A and angle θ_B to section A, $y''_A = y_B + \theta_B L_1$. The deflection and misalignment angle of position A can be written as

$$y_A = \frac{F}{3E}\left(\frac{L_1^3}{I_1} + \frac{L_2^3 - L_1^3}{I_2}\right), \tag{5}$$

$$\theta_A = \frac{F}{2E}\left(\frac{L_1^2}{I_1} + \frac{L_2^2 - L_1^2}{I_2}\right). \tag{6}$$

2.2 Angle of journal misalignment of a complex rotor

Eqs. (5) and (6) are suitable for a shaft with two steps. However, the rotor system usually needs to meet requirements, and is processed with many steps. Following a derivation similar to the above process, the deflection and misalignment angle of a shaft with n steps are given by

$$y = \frac{F}{3E}\left(\frac{L_1^3}{I_1} + \frac{L_2^3 - L_1^3}{I_2} + \frac{L_3^3 - L_2^3}{I_3} + \cdots + \frac{L_n^3 - L_{n-1}^3}{I_n}\right), \tag{7}$$

$$\theta = \frac{F}{2E}\left(\frac{L_1^2}{I_1} + \frac{L_2^2 - L_1^2}{I_2} + \frac{L_3^2 - L_2^2}{I_3} + \cdots + \frac{L_n^2 - L_{n-1}^2}{I_n}\right). \tag{8}$$

Apart from many simple rotors, many complex rotors can also be simplified as a step shaft or be given their own deflection and misalignment formulation to

analyze the lubrication (Fig. 3). Timoshenko and Gere (1972) proposed a method for computing the deflection angle of a simple shaft. Liu (1994) gave the deflection and angle of a shaft with two steps, and also introduced overlay method theory. Xu and Li (1982) analyzed the section of initial moment and stiffness of complex structures, such as crankshafts, or cone structures.

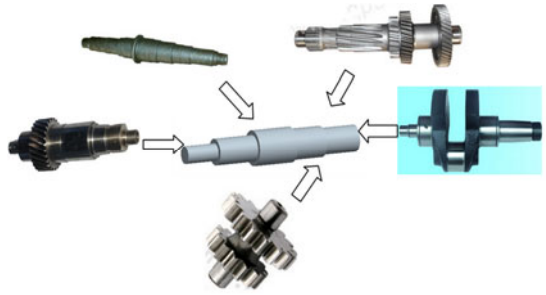

Fig. 3 Misalignment deflection and angle equivalent

When a rotor has an asymmetric structure, the asymmetric characteristic causes another angle component, and this angle is always neglected in lubrication analysis. The contribution of this angle is the reason for deflection asymmetry (Fig. 4). Based on Eqs. (7) and (8), the misalignment angles of A and G positions need to be reduced or increased by the angle caused by asymmetry deflection. The misalignment angles of positions A and G are then $\theta_A = \theta'_A - \theta'$ and $\theta_G = \theta'_G + \theta'$, respectively. These angle components can be written as follows:

$$\tan\theta' = \frac{y_A - y_G}{L'}, \tag{9}$$

where $L' = L'_3 + L_4$, y_A is the deflection of position A, and y_G the deflection of position G, where L_1, L_2, L_3, L_4, L'_1, L'_2, and L'_3 are the lengths of every beam as shown in Fig. 4.

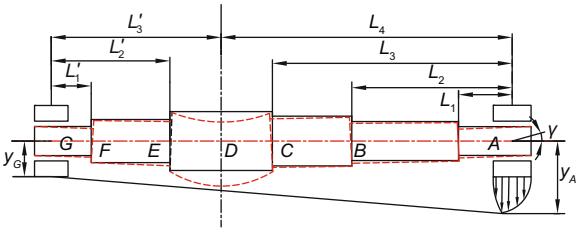

Fig. 4 Misalignment angle model analysis with a complex rotor

2.3 Oil film thickness

When misalignment happens, the value of the misalignment angle can be obtained by the above method. This subsection describes the governing equations for the lubrication of a tilting-pad journal bearing assuming elastic and thermal effects. The film thickness in case of a journal misalignment inside the bearing as shown in Fig. 5 can be defined by

$$h = c + e\cos(\theta - \varphi) + \tan\gamma\left(y - \frac{L}{2}\right)\cos(\theta - \alpha - \varphi), \tag{10}$$

where c is the clearance of the bearing, e is the eccentricity at the bearing middle section, L is the length of the bearing, γ is the misalignment angle, φ is the angle between the load line and the line of centers, α is the angle between φ and the rear center of the misaligned journal. In Fig. 5, C_1, C_2, and C_3 are intersections of the journal axis with the front, middle, and rear planes of the bearing, and e' is the magnitude of the projection of the axis of the misaligned journal on the midplane of the bearing. As shown in Fig. 4, M_x and M_z is the component of misalignment moment along x- and z-direction, respectively, W_x and W_z is the component of load capacity along x- and z-direction, respectively.

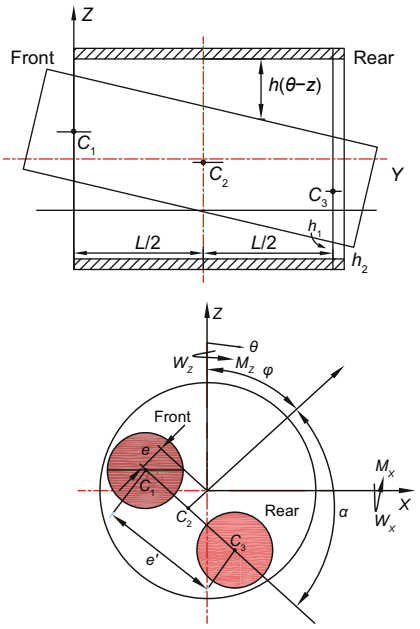

Fig. 5 Misaligned journal bearing system

2.4 Generalized Reynolds equation

On the basis of conventional assumptions of lubrication theory, the generalized Reynolds equation with film thickness is

$$\frac{\partial}{\partial\theta}\left(F_2\frac{\partial p}{\partial\theta}\right)+\frac{\partial}{\partial y}\left(F_2\frac{\partial p}{\partial y}\right)=\frac{\partial}{R\partial\theta}\left[U\left(h-\frac{F_1}{F_0}\right)\right], \quad (11)$$

where p is the oil film pressure, U is the velocity of the journal, $F_2=\int_0^h z(z-F_1/F_0)/\eta\mathrm{d}z$, $F_1=\int_0^h z/\eta\mathrm{d}z$, and $F_0=\int_0^h 1/\eta\mathrm{d}z$. F_2, F_1, and F_0 all contain the viscosity η, and are in integration form. The Simpson rule is used to solve this characteristic, so every integration item can be written as

$$S_n=\frac{h'}{6}\left[f(a')+4\sum_{k'=0}^{n'-1}f(x_{k'+1/2})+2\sum_{k'=1}^{n'-1}f(x_{k'})+f(b')\right], \quad (12)$$

where $f(a')$ and $f(b')$ are the boundary values in the range, and $f(x_{k'+1/2})$ and $f(x_{k'})$ are the even and odd point values, respectively.

There is a significant correlation among temperature, viscosity, and pressure, when the oil film pressure is high. The effect of pressure on the oil film viscosity is significant. In this study, the oil sample CD30 is used for the analysis, and the viscosity in Eq. (13) follows the viscosity-temperature-pressure relationship suggested by Roelands (2002):

$$\eta=\eta_0\exp\left\{(\ln\eta_0+9.67)\times\left[(1+5.1\times10^{-9}p)^{0.68}\left(\frac{T-138}{T_0-138}\right)^{-1.1}-1\right]\right\}, \quad (13)$$

where T_0=300 K and η_0=0.1193 Pa·s. According to Eq. (13), the viscosity in the oil inlet is 0.0649 Pa·s.

Vogel's equation describes the variation of oil viscosity with temperature, in which the viscosity-pressure variation is not considered. Vogel's equation is defined as

$$\eta=\lambda_1\exp[\lambda_2/(T-T_1)], \quad (14)$$

where $\lambda_1=0.5076\times10^{-3}$ and λ_2=3434.6 are the temperature-viscosity coefficients, and T_1=22.29 K is the temperature constant. In the oil inlet the viscosity is 0.0686 Pa·s, so the viscosity in the two models is nearly the same as in the oil inlet position.

The pressure flow term in the θ-direction is

$$\begin{aligned}\frac{\partial}{R\partial\theta}\left(F_2\frac{\partial p}{R\partial\theta}\right)_{i,j}&=\frac{1}{R^2\Delta\theta}\left[\left(F_2\frac{\partial p}{\partial\theta}\right)_{i+\frac{1}{2},j}-\left(F_2\frac{\partial p}{\partial\theta}\right)_{i-\frac{1}{2},j}\right]\\&=\frac{1}{R^2\Delta\theta^2}\left\{\frac{1}{2}[(F_2)_{i,j}+(F_2)_{i+1,j}](p_{i+1,j}-p_{i,j})-\frac{1}{2}[(F_2)_{i,j}+(F_2)_{i-1,j}](p_{i,j}-p_{i-1,j})\right\}\\&=\frac{1}{2R^2\Delta\theta^2}\{[(F_2)_{i,j}+(F_2)_{i+1,j}]p_{i+1,j}-[2(F_2)_{i,j}+(F_2)_{i+1,j}+(F_2)_{i-1,j}]p_{i,j}+[(F_2)_{i,j}+(F_2)_{i-1,j}]p_{i-1,j}\},\end{aligned} \quad (15)$$

where $\Delta\theta$ is equal to $2\pi/m$, and R is the radius of the bearing.

The integration part can be transformed into a polynomial equation. A decomposition method is used to solve it, and the Reynolds Eq. (11) can be expressed as

$$a_{i,j}^1p_{i,j-1}+a_{i,j}^2p_{i-1,j}+a_{i,j}^3p_{i,j}+a_{i,j}^4p_{i+1,j}+a_{i,j}^5p_{i,j+1}=a_{i,j}^0, \quad (16)$$

where $a_{i,j}^1$, $a_{i,j}^2$, $a_{i,j}^3$, $a_{i,j}^4$, and $a_{i,j}^5$ are the coefficients of the pressures $p_{i,j-1}$, $p_{i-1,j}$, $p_{i,j}$, $p_{i+1,j}$, and $p_{i,j+1}$, respectively, and $a_{i,j}^0$ is a constant.

The pressure is calculated by using the virtual meshes located in θ=0 and θ=2π. The pressure boundary conditions are given by

$$\begin{cases}p(\theta,0)=p(\theta,L)=0,\\p(\theta_1,0)=p',\\p(\theta_2,0)=\dfrac{\partial(\theta_2,0)}{\partial\theta}=0,\end{cases} \quad (17)$$

where p' is the pressure at the oil supply point, θ_1 is the oil supply of the hydrodynamic film, and θ_2 is the cavitation point of the hydrodynamic film.

The whole mesh region is divided into three parts: (1) The center (the mesh $(2-m-1)\times(2-n-1)$); (2) The edges (i=1, j=2−m−1; i=n, j=2−m−1; j=1,

i=2−n−1; j=m, i=2−n−1); (3) Four corner points (i=1, j=1; i=1, j=m; j=1, i=n; j=m, i=n). In this study, n=31 and m=101. However, when the bearing unfolds, one part is connected to the other side, so the virtual mesh is introduced.

2.5 Energy equation

According to the conservation of energy, volume force and radiation are neglected. Compared with the length along the x- and y-direction, the thickness of the oil film is very small, and thus the thermal conduction along the x- and y-direction is neglected. The velocity w along the oil film direction is also very small, and can be neglected (w=0). The energy equation can be written as

$$\rho c_{\mathrm{f}}\left(u\frac{\partial T}{R\partial\theta}+v\frac{\partial T}{\partial y}+w\frac{\partial T}{\partial z}\right)=K_{\mathrm{f}}\frac{\partial^2 T}{\partial^2 x}+K_{\mathrm{f}}\frac{\partial^2 T}{\partial^2 y}+K_{\mathrm{f}}\frac{\partial^2 T}{\partial^2 z}+\eta\left[\left(\frac{\partial u}{\partial z}\right)^2+\left(\frac{\partial v}{\partial z}\right)^2\right], \tag{18}$$

where ρ is the density of the oil film, u, v, and w are the components of the oil film velocity in the circumferential, width, and radial directions, respectively, c_{f} is the specific heat of the oil film, K_{f} is the thermal conductivity of the oil film, and T is the oil film temperature.

The velocity u, v gradients along the z-direction are given by

$$\frac{\partial u}{\partial z}=\frac{1}{\eta}\frac{\partial p}{\partial x}z-\frac{U}{h}-\frac{\partial p}{\partial x}\frac{h}{2\eta}, \tag{19}$$

$$\frac{\partial u}{\partial z}=\frac{1}{\eta}\frac{\partial p}{\partial x}z-\frac{U}{h}-\frac{\partial p}{\partial x}\frac{h}{2\eta}. \tag{20}$$

2.6 Heat conduction equation

The temperature field in the bearing is computed by solving the heat conduction equation in cylindrical coordinates. Both the bearing and housing are assumed to be circular rings along the thickness direction. The heat transfer equation can be defined as

$$\frac{\partial^2 T_{\mathrm{B}}}{\partial r_{\mathrm{B}}^2}+\frac{1}{r_{\mathrm{B}}}\frac{\partial^2 T_{\mathrm{B}}}{\partial r_{\mathrm{B}}^2}+\frac{1}{r_{\mathrm{B}}^2}\frac{\partial^2 T_{\mathrm{B}}}{\partial\theta^2}+\frac{\partial^2 T_{\mathrm{B}}}{\partial z^2}=0, \tag{21}$$

where T_{B} is the temperature of the bearing bush.

2.7 Velocity and leakage equations

u and v are the integration of $\frac{\partial u}{\partial z}$ and $\frac{\partial v}{\partial z}$ with two constants C_1' and C_2'. The two constants can be solved based on the boundary conditions, where the velocities of the shaft and bearing surface are U and 0, respectively. When z=0, u=U, and z=h, u=0, the velocity of the oil film along the x- and y-direction can be written as follows:

$$u=\frac{1}{2\eta}\frac{\partial p}{\partial x}(z^2-zh)-U\frac{z}{h}, \tag{22}$$

$$v=\frac{1}{2\eta}\frac{\partial p}{\partial y}(z^2-zh). \tag{23}$$

The lubricant flow rate Q_1 from the front-end plane and the lubricant flow rate Q_2 from the rear-end plane of the bearing are given by

$$Q_1=\int_0^h\int_0^{2\pi}\frac{h^3}{12\eta}\cdot\left.\frac{\partial p}{\partial y}\right|_{y=0}R\mathrm{d}\theta\mathrm{d}z, \tag{24}$$

$$Q_2=\int_0^h\int_0^{2\pi}\frac{h^3}{12\eta}\cdot\left.\frac{\partial p}{\partial y}\right|_{y=L}R\mathrm{d}\theta\mathrm{d}z. \tag{25}$$

2.8 Boundary condition

Deng (2008) proposed that the temperature of every position is strongly related to the upstream point, but has little relationship to the downstream point. The phenomenon of backward flow exists at the point of entry, so the temperature along the circumference direction satisfies the followings:

$$\begin{cases}\left(\dfrac{\partial T}{\partial\theta}\right)_{i,j,k}=\dfrac{1}{\Delta\theta}(T_{i,j,k}-T_{i-1,j,k}), & u\geq 0,\\ \left(\dfrac{\partial T}{\partial\theta}\right)_{i,j,k}=\dfrac{1}{\Delta\theta}(T_{i+1,j,k}-T_{i,j,k}), & u<0.\end{cases} \tag{26}$$

As well as exchanging heat with the shaft, the oil film also exchanges heat with the bearing bush and heat conduction occurs in the bearing bush.

The temperature in the oil supply hole can be written as

$$T=T_{\mathrm{in}}. \tag{27}$$

The temperature in the fluid in contact with the journal interface can be written as

$$k_o \left.\frac{\partial T}{\partial r}\right|_{r=R} = -k_f \left.\frac{\partial T}{\partial z}\right|_{z=h}. \tag{28}$$

The boundary condition of the bush lateral surface can be defined as

$$k_o \left.\frac{\partial T}{\partial z}\right|_{z=0,L} = h'(T|_{y=0,L} - T_a). \tag{29}$$

The boundary condition of the bush outside surface can be expressed as

$$k_o \left.\frac{\partial T}{\partial r}\right|_{r=R_2} = h'(T|_{r=R_2} - T_a), \tag{30}$$

where T_{in} is the temperature of the oil supply, T_a is the ambient temperature, k_o and k_f are the thermal conductivity, h' is the heat convective coefficient, and R_2 is the radius of the bush outside.

2.9 Genetic theory to analyze the parameters

The misalignment angle for two bearings is a problem of multi-objectives. In this study, the genetic optimization method is used, and the aim can be written as

$$\begin{aligned} &\min f_1 = \min(\theta_G + \theta'), \\ &\min f_2 = (\theta_A - \theta'), \\ &\text{s.t.} \quad a \le D \le b, A \le L \le B, \end{aligned} \tag{31}$$

where f_1 and f_2 are the objective functions, a, b is the lower and upper limit of each diameter, respectively, and A, B is the lower and upper limit of each length, respectively.

Using the genetic method, the effect of every parameter and the best results can be obtained easily. Fig. 6 presents a simulation result from genetic theory based on the rotor parameters, assuming that the diameters and lengths of every step are in the ranges of $a \le D \le b$ and $A \le L \le B$, respectively. The analysis results show that the misalignment angle is the smallest when $D=b$, $A=L$, and $d_0=0$. Although the result can be easily related to the structure, more complex rotors, such as a crankshaft, need more research and the contributions of all structural components need to be considered.

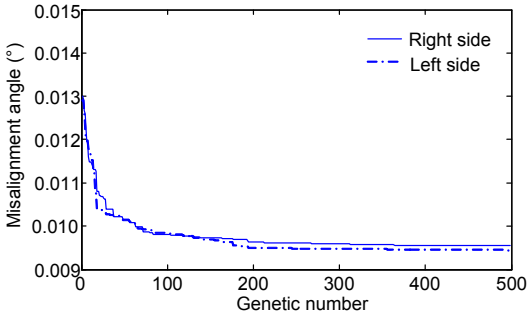

Fig. 6 Genetic analysis for the misalignment angle

3 Numerical processes

The complex rotor can be simplified as a simple step shaft problem, according to Eqs. (7)–(9). The deflection and misalignment angle caused by deformation can then be calculated. Genetic theory is used to investigate the effects of parameters of structure on the misalignment angle. Coupling the structure characteristics with lubrication, a five-point central difference method is used to solve the Reynolds equation and energy equation. The whole process is shown in Fig. 7.

A mesh of the oil film is created in the thickness and circular directions. The Reynolds equation is solved iteratively using the successive over relaxation method. The pressure, temperature, and viscosity need to satisfy the convergence with the initial guess until the switching functions are determined:

$$\begin{cases} \dfrac{\left|p_{i,j}^{n+1} - p_{i,j}^{n}\right|}{p_{i,j}^{n+1}} \le 10^{-4}, \\ \dfrac{\left|T_{i,j}^{n+1} - T_{i,j}^{n}\right|}{T_{i,j}^{n+1}} \le 10^{-4}, \\ \dfrac{\left|\eta_{i,j,k}^{n+1} - \eta_{i,j,k}^{n}\right|}{\eta_{i,j,k}^{n+1}} \le 10^{-4}. \end{cases} \tag{32}$$

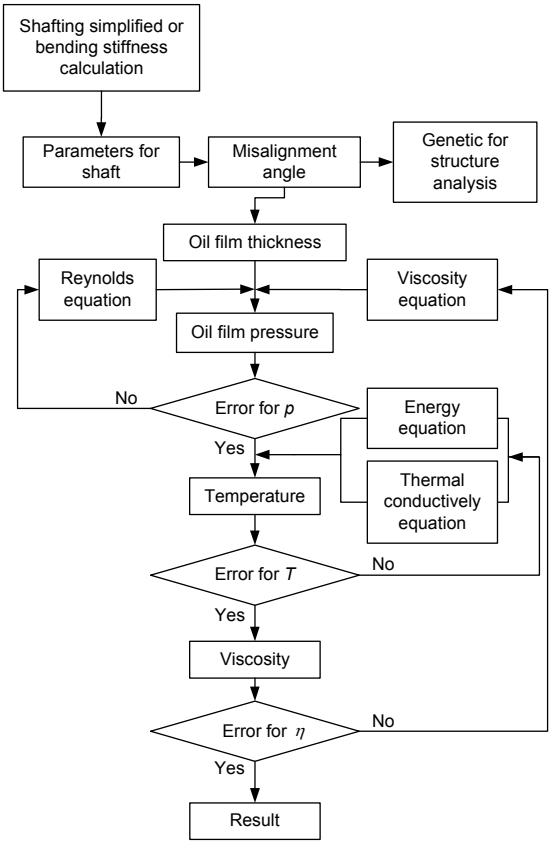

Fig. 7 Flow chart of the analysis

4 Results and discussion

4.1 Model description

The rotor-bearing system used in this study is shown in Fig. 8. A flexible shaft is supported by two bearings, and the load of the bearing is a nonlinear oil film force. Based on this system, the severity of misalignment can be represented by all the structure parameters. The parameters of the shaft shown in Table 1 were used to investigate the effect of parameters on the misalignment angle. Parameters such as the exciting load F and the radius of the hollow part d_0 were investigated.

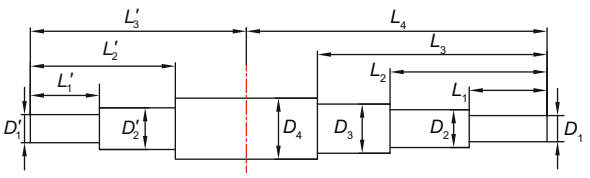

Fig. 8 Structure of the step shaft

Apart from the misalignment angle analysis, the misalignment analysis was carried out in combination with lubrication theory. Lubrication parameters are shown in Table 2.

Table 1 Parameters of rotor

Parameter	Value (m)	Parameter	Value (m)
D_1	0.050	d_0	0
D_2	0.055	L_1	0.040
D_3	0.065	L_2	0.120
D_4	0.080	L_3	0.150
D_0'	0	L_4	0.190
D_1'	0.050	L_1'	0.040
D_2'	0.060	L_2'	0.080
D_3'	0.080	L_3'	0.120

Table 2 Lubrication parameters

Parameter	Value
Speed (rad/min)	3000
Clearance (m)	3×10^{-5}
Oil density (kg/cm^3)	860
Elastic module (GPa)	210
Journal radius (m)	0.025
Ambient temperature (K)	313
Thermal conductivity of lubricant (W/(m·K))	0.13
Specific heat of lubricant (J/(kg·K))	2000
Initial bearing width (m)	0.05
Oil supply temperature (K)	313
Thermal conductivity of bush housing (W/(m·K))	250
Heat transfer coefficient of bush housing (W/(m^2·K))	80
Thermal conductivity of journal (W/(m·K))	50

4.2 Validation

Sun and Gui (2004) worked on a misaligned journal bearing, and described the maximum pressure as a function of the eccentric ratio at a fixed bearing load. The input data follows our bearing parameters. Fig. 9 shows the maximum pressure found in this study and from their theory. The misalignment angle was 0.007°. The results of the present work are in good agreement with Sun and Gui (2004)'s theory. The prediction of the maximum oil film pressure (MOFP) was slightly lower than those from simulation results

by Sun and Gui (2004) when the eccentric ratio was less than 0.7. When the eccentric ratio was larger than 0.8, the prediction of the MOFP was higher than those from simulation results by Sun and Gui (2004). We expect that these differences arose from the neglect of temperature and viscosity differences, and from some assumptions about boundary conditions. The comparison also found that if the viscosity is constant, it is hard to define the constant value, and has a great effect on the MOFP prediction.

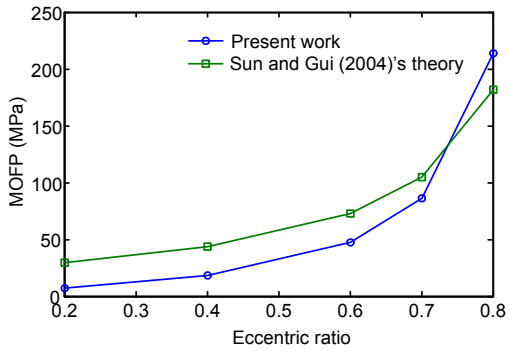

Fig. 9 Model validation

4.3 Misalignment angle analysis

Rotor design always focuses separately on strength and lubrication analysis. In fact, lubrication must be combined with structure to analyze the lubrication. Oil film thickness is determined by clearance, misalignment angle, bearing width, and two angle parameters. However, it is hard to define angles α and φ. Further research is needed to understand how the angles α and φ change. According to the structure parameters of the rotor, an increase in the exciting force leads to an increase in misalignment. However, previous studies focused only on symmetrical rotors or did not even consider the rotor. If the rotor system is not symmetrical, the load is distributed differently, and an asymmetrical rotor can cause the lubrication characteristics to be different. When the other parameters are constant, the exciting load has a linear relationship with the misalignment angle. An increasing load can lead to increased misalignment, and an asymmetrical structure can cause another misalignment angle component which is added to or subtracted from the initial angle.

Misalignment angles under different exciting load conditions are shown in Fig. 10. Although the asymmetry deflection is considered, the misalignment angle still has a linear relationship with the exciting load. With an increase in the exciting load, the error between the misalignment angles, both considering and not considering deflection asymmetry, increases. Misalignment angles are nearly the same after deflection asymmetry is considered.

To save material or satisfy design demands, rotors are designed to be hollow. Misalignment angles under different hollow diameters d_0 are shown in Fig. 11. The exciting load F is 8000 N. The change in the misalignment angle with the hollow diameter d_0 shows that when d_0 is smaller than 20 mm, it has little effect on the lubrication characteristics. If the rotor satisfies strength demand, it not only can save material, but also cannot influence the lubrication. When d_0 changes from 20 mm to 30 mm, misalignment angle changes slightly. When d_0 is larger than 30 mm, misalignment angle changes greatly. Thus, other parameters such as the diameter of every step and the length of every step, which have effects on lubrication, are also worth looking into as they may enable large savings in material. The deflection, misalignment angle, and the angle that is caused by asymmetry

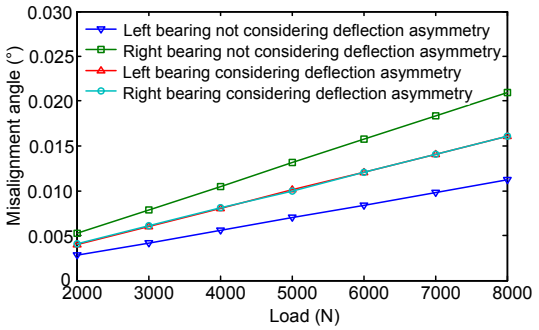

Fig. 10 Asymmetry deflection influences the misalignment under different loads

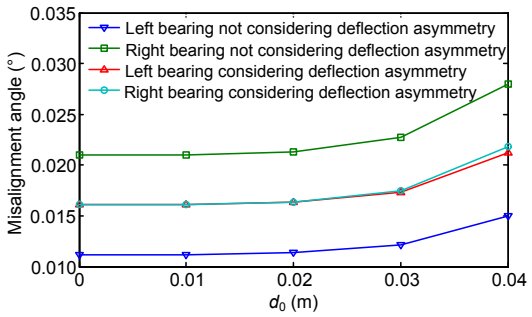

Fig. 11 Asymmetry deflection influences the misalignment under different d_0

deflection are shown in Table 3. The result shows that their contributions cannot be neglected.

4.4 Oil film thickness analysis

The effects of journal misalignment and the orientation of journal misalignment on bearing lubrication performance when journal misalignment takes place in the bearing caused by asymmetry deflection were analyzed. According to the factual load acting on the rotor, α=0, φ=0, e=2.1×10^{-5} m, and d_0=0. The exciting force is equal to 8000 N, so the loads distributed to the right and left bearings are 3096.8 N and 4903.2 N, respectively. The oil film thickness distribution on the both sides of the bearing where the asymmetry deflection is considered is shown in Fig. 12. When the asymmetry deflection is considered, the misalignment angles of the left and right bearings are the same and equal to 0.0161°, on two sections such as n=1 and n=31 that are at the rear and front of the bearing, respectively. The results show that at the rear the oil film thickness of the right bearing that does not consider the asymmetry deflection tends to be zero, and serious asperity contact occurs in these regions. However, when the asymmetry deflection is considered, the minimum oil film thickness (MOFT) increases, but at the front, the oil film thickness of the right bearing that does not consider deflection asymmetry is larger than in any other condition. The oil film thickness inclines to one side because of the misalignment angle, if that side does not consider the asymmetry deflection, and it will underestimate or overestimate the MOFT (Fig. 12b).

According to Table 3, when d_0=0, the misalignments of the left and right bearings are both 0.0161°. The changes in MOFT with changes in the bearing width under different eccentric ratios are shown in Fig. 13. Combined with Fig. 5, when the misalignment angle is known, with a decrease in the bearing width, the MOFT increases (Fig. 5, h_1>h_2), so the results coincide.

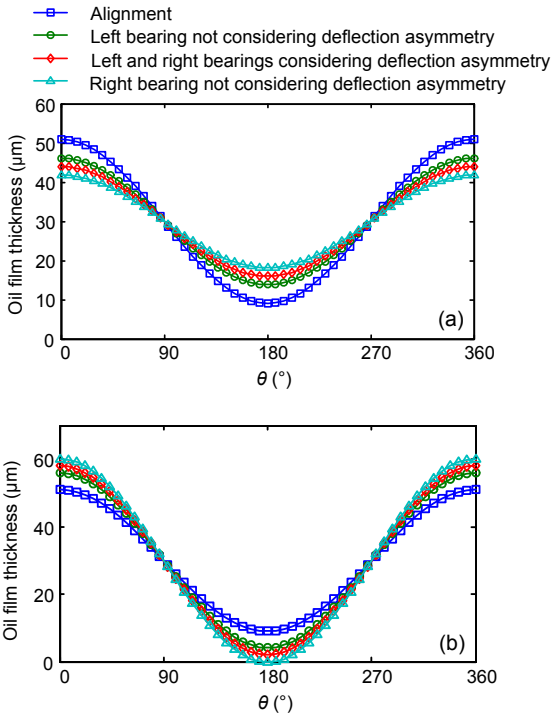

Fig. 12 Asymmetry deflection influences the oil film thickness
(a) Front side; (b) Rear side

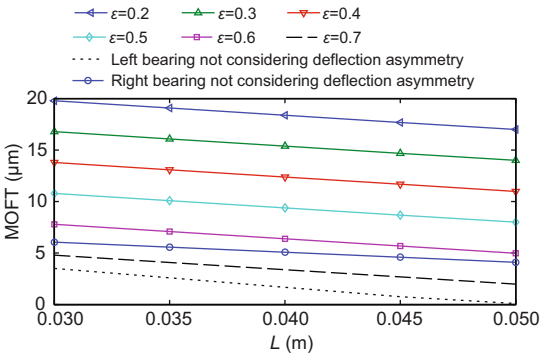

Fig. 13 MOFT changes with bearing width

Table 3 Shaft deformation influenced by d_0

d_0 (m)	Shaft deformation						
	y_A (m)	y_G (m)	θ' (°)	θ_A' (°)	θ_G' (°)	θ_A (°)	θ_G (°)
0	3.884×10^{-5}	1.240×10^{-5}	0.0049	0.02100	0.01120	0.01610	0.01610
0.01	3.887×10^{-5}	1.241×10^{-5}	0.0049	0.02102	0.01120	0.01612	0.01610
0.02	3.933×10^{-5}	1.254×10^{-5}	0.0050	0.02132	0.01136	0.01632	0.01636
0.03	4.150×10^{-5}	1.314×10^{-5}	0.0052	0.02270	0.01211	0.01750	0.01731
0.04	4.924×10^{-5}	1.533×10^{-5}	0.0062	0.02800	0.01500	0.02180	0.02120

Thus, the initial bearing width (L×D=50 mm× 50 mm) may cause asperity contact. In the analysis below, the bearing width is changed to 40 mm to analyze temperature, velocity and oil leakage. From the above analysis, if the asymmetry deflection is neglected, the design of the bearing may be faulty. However, all the lubrication prediction mistakes come from errors in MOFT which are the direct cause of errors in the analysis of the lubrication.

4.5 Effect of load and bearing width on lubrication analysis

In the bearing design above, asperity may occur in the lubrication, so suitable bearing parameters, such as the load and bearing geometry, are very important in the process of bearing design. The design needs to satisfy some rules: it must avoid asperity contact, meet the load capacity, the oil temperature cannot be too high, etc. Fig. 14 presents the effect of different bearing widths and loads on the MOFP when the misalignment angle equals 0.0161°. The result shows that when the bearing width increases, the MOFP increases, especially when ε (ε=e/c)=0.7.

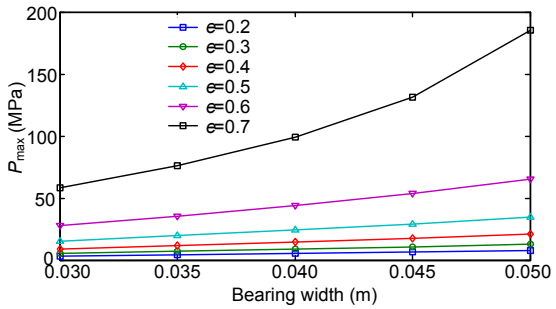

Fig. 14 MOPF changes with bearing width at different eccentric ratios

Apart from the bearing geometry, the exciting load and speed also have a great effect on lubrication characteristics. We analyzed the relationship between the MOFP and load and the relationship between the MOFP and speed (Fig. 15). When the asymmetry deflection was considered, the misalignment angle is 0.0161°, but if this component is neglected, the misalignment angles of the right and left bearings are 0.021° and 0.0112°, respectively. The results show that with increasing load and speed, the MOFP increases. When the asymmetry deflection is considered, the error increases with the load and speed, so the asymmetry has a great effect on the prediction of MOFP, and a suitable load and speed is very important when the bearing is designed.

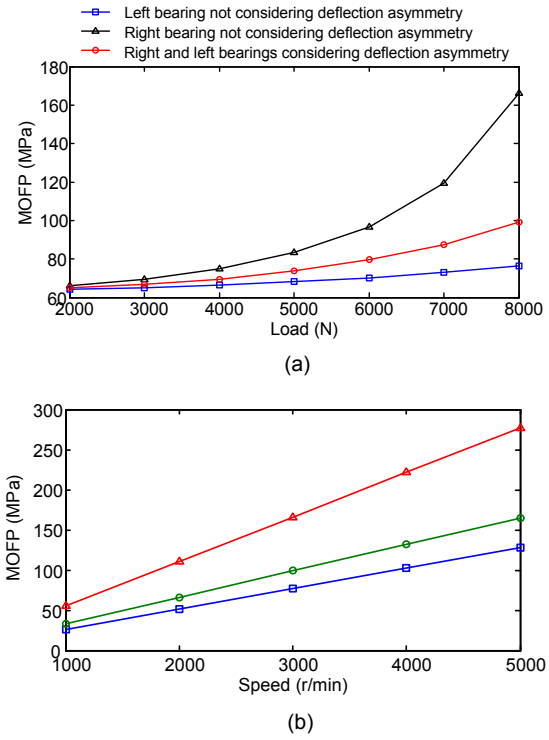

Fig. 15 MOFP changes with load (a) and speed (b) (L×D=40 mm×50 mm, ε=0.7)

4.6 Oil film pressure analysis

The angle α influences the oil film distribution, when the angle φ is defined. The angle α adds to or reduces an angle, the whole pressure moves along the circumference direction, and the amplitude does not change. The angle φ changes the shape of the oil film distribution. When the angle φ equals π/2, a special oil film pressure distribution will appear. An increasing misalignment angle will lead to two peak values and the shape will be oblique along the width direction. If φ is smaller than π/2, the oil film pressure inclines to the rear of the bearing. If φ is bigger than π/2, the oil film pressure inclines to the front of the bearing.

According to the analysis above, the misalignment angle, angles α and φ, and eccentric e are four factors influencing the oil film thickness. The influence of these factors on the lubrication characteristics was investigated. Fig. 16 shows the effect of the angle component of asymmetry deflection on the oil film

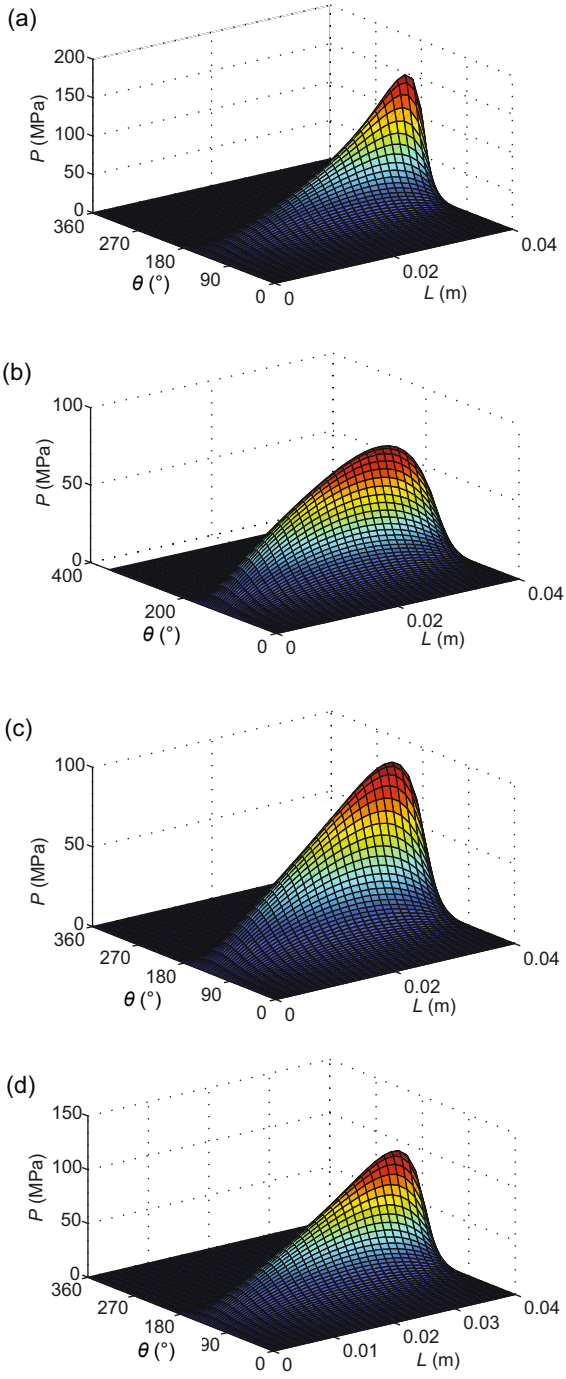

Fig. 16 Effect of asymmetry deflection on oil film pressure distribution (φ=0, e=2.1×10^{-5}, d_0=0, α=0, and L=40 mm)

(a) Right bearing not considering the asymmetry deflection; (b) Left bearing not considering the asymmetry deflection; (c) Right and left bearings considering the asymmetry deflection when γ=0.0161°; (d) Right and left bearing considering the asymmetry deflection when γ=0.0175°

pressure distribution of two bearings. Fig. 16a presents the oil film pressure of the right bearing. The pressure inclines to one side, and the maximum pressure does not occur at an angle of 180°, but at 172.8°. The MOFP is 166.1 MPa. The MOFP of the left bearing is 76.9 MPa, and occurs at 162°. When the asymmetry deflection is considered, and the misalignment angles of the left and the right bearings are both 0.0161°, the maximum pressure is 99.1 MPa, and its position is 165.6°. Thus, the left and right bearings cause errors that can reach 67 MPa and −22.2 MPa, respectively, so it is very important to consider the asymmetry deflection or a larger error may occur. When the hollow diameter d_0 increases to 0.03 m, the misalignment angles of the left and right bearings both increase to 0.0175°, the oil pressure increases to 110.5 MPa, and its peak position is at 169.2°.

4.7 Oil film velocity and oil leakage

To analyze the oil leakage more thoroughly, the bearing leakage at the front and at the rear were compared. The average leakage of the bearing under different speeds and bearing widths was also compared (Fig. 17). The result shows that as the eccentric ratio increases, the leakage increases, but the effects on the front and rear are different. The largest effect is located at the point to which the pressure is inclined. The misalignment angle has little effect on the leakage, and the sum of the leakage is nearly the same. When the bearing width decreases the oil leakage decreases, too. With increasing speed, the oil leakage increases. So it is also very important to consider the oil leakage in combination with a suitable bearing width and speed.

The velocity of the oil film along the y direction is the key factor in the oil flow leakage. The oil film is

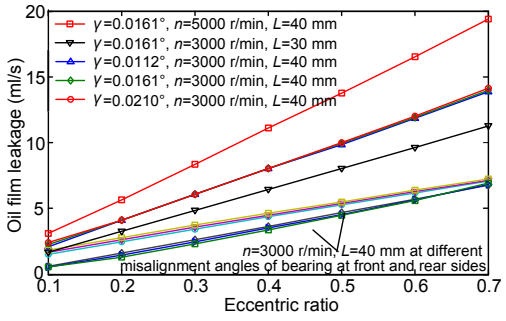

Fig. 17 Oil leakage changes with the eccentric ratios

also meshed with k points along the oil film thickness direction. The velocity v when k=6 is shown in Fig. 18.

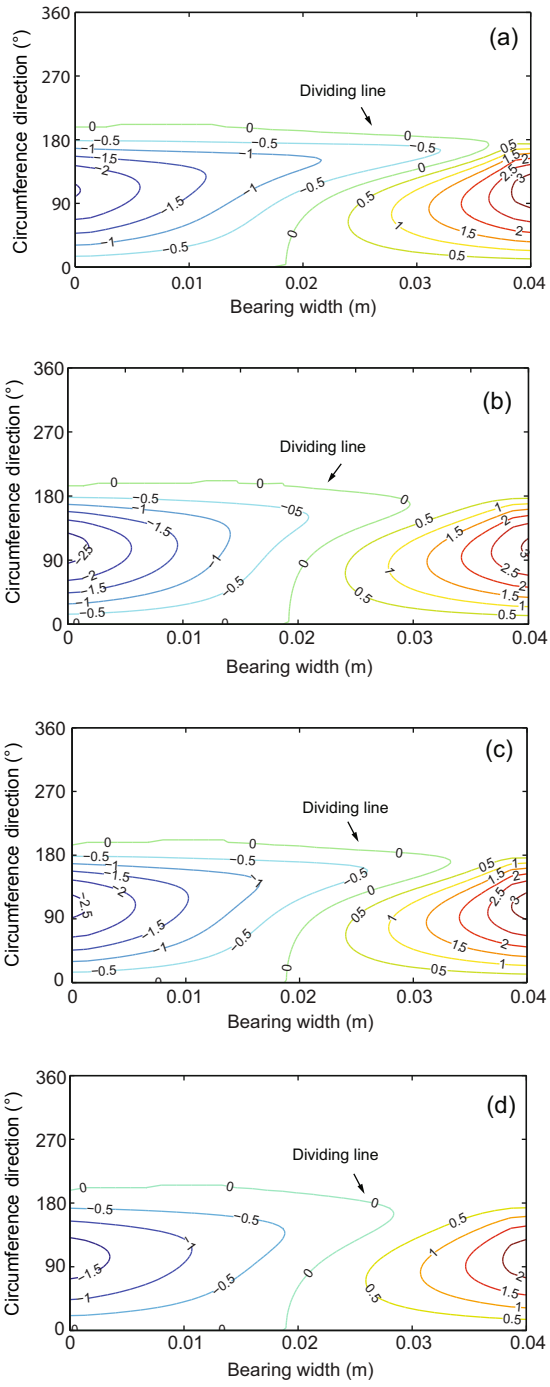

Fig. 18 Velocity comparison

(a) Right bearing not considering the asymmetry deflection; (b) Left bearing not considering the asymmetry deflection; (c) Left bearing considering the asymmetry deflection; (d) Left bearing considering the asymmetry deflection, but ε=0.5

The results show that when the eccentric ratio equals 0.7 (Fig. 18a–18c), the misalignment angles are 0.021°, 0.0112°, and 0.0161°, respectively. The velocities v are nearly the same, and the maximum velocity is 3 m/s at the point to which the pressure is inclined. But the other side velocity v is also very large, and all the velocity distribution is nearly the same. The maximum velocity can reach 2.5 m/s. However, when the eccentric ratio equals 0.5 (Fig. 18d), the misalignment angle equals 0.0161° and does not change. The maximum velocity v changes greatly. It decreases to 2 m/s, leading to a decrease in the oil leakage. The dividing line for the velocity v also changes: when the pressure inclines steeply to the front, the dividing line also inclines to that side and the gradient becomes denser. As no more oil film can pass through the bearing and flow out, it is bad for lubrication.

The leakage and velocity distributions along the circumference are shown in Fig. 19. The result shows that the maximum leakage occurs earlier than the maximum velocity.

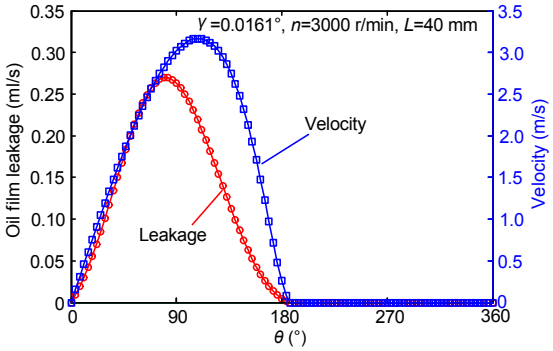

Fig. 19 Velocity and leakage distribution

According to the average oil leakage analysis (Fig. 17), the oil leakage is nearly the same when the misalignment angle changes, but the eccentric ratio can change the oil film leakage significantly. The oil leakage distribution along the bearing width direction is shown in Fig. 20. The results show that at the rear, the discretion oil leakage of the right bearing, not considering the asymmetry deflection along the bearing width direction, is larger than under any other conditions. However, at the front, it is smaller than under any other conditions. So together the results

explain why the average oil leakage is the same although the misalignment angle is different.

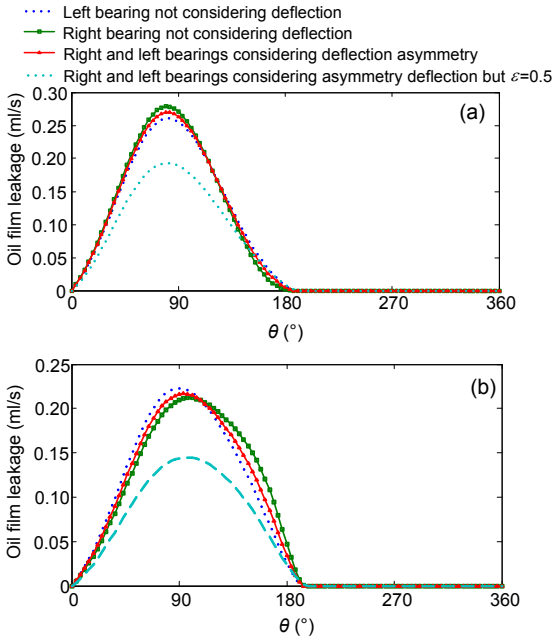

Fig. 20 Leakage discretization
(a) Rear side; (b) Front side

4.8 Viscosity analysis

In this study, the influence of pressure and temperature on oil film is analyzed (Fig. 21b). To find the effect of pressure on the viscosity, the η-T model is also used in this problem (Fig. 21a). The oil viscosity is very large in the oil inlet position because of the low temperature. As temperature increases, the average velocity of the fluid molecules increases, and molecular distances between them increase. This causes the viscosity to decrease. To analyze the viscosity thoroughly, the pressure cannot be neglected, especially at high pressure. Wen and Huang (2002) showed that when the pressure reaches 1–10 GPa, the viscosity can increase significantly. It is very important to consider the effect of pressure, especially at bigger loads. According to our results (Fig. 21), the viscosity in higher pressure regions will increase, but when the effect of pressure is neglected, the values decrease. So it is very important to consider the relationship between viscosity and pressure. This result will also influence some other lubrication characteristics such as the oil film pressure. For example, if the η-T model is used to analyze lubrication with the parameters the same as shown in Fig. 16b, unlike the result above, the maximum pressure is 83.2 MPa. To find the detailed difference, viscosity at the maximum oil film pressure position based on the P-η-T model and the η-T model of the position are compared. The results show that the maximum oil film pressure occurs at the same position, but the values are 0.05965 Pa·s and 0.01567 Pa·s for the P-η-T model and η-T model, respectively. Thus, it is very important to consider the effect of oil film pressure.

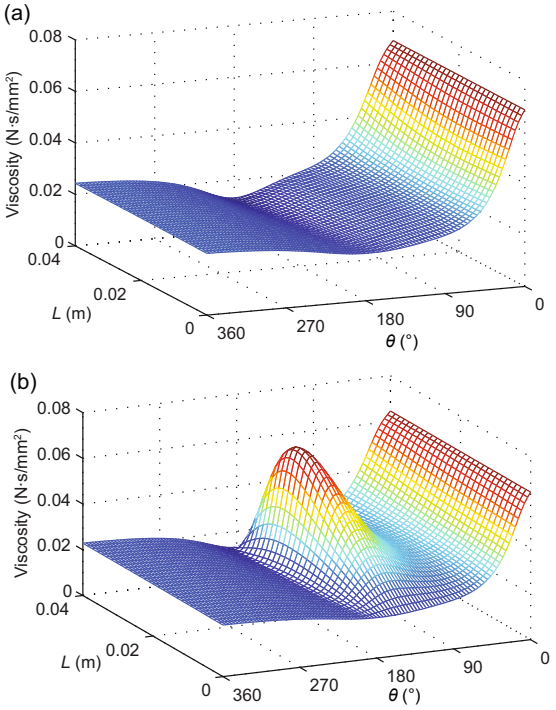

Fig. 21 Viscosity distribution under different models at one section k=8 (φ=0, e=2.1×10^{-5}, d_0=0, L=40 mm, γ=0.0112°)
(a) η-T model; (b) P-η-T model

4.9 Temperature field analysis

Fig. 22 presents the effects of asymmetry deflection on the temperature distribution. The section is along the thickness direction k=10. Combining with Fig. 16, the results show that the temperature increases suddenly until the peak pressure position reaches and then the pressure drops. The temperature also drops until the pressure is zero, and then the temperature is constant. However, the temperature distribution is similar under different conditions (Fig. 22). Fig. 22a shows that maximum temperature

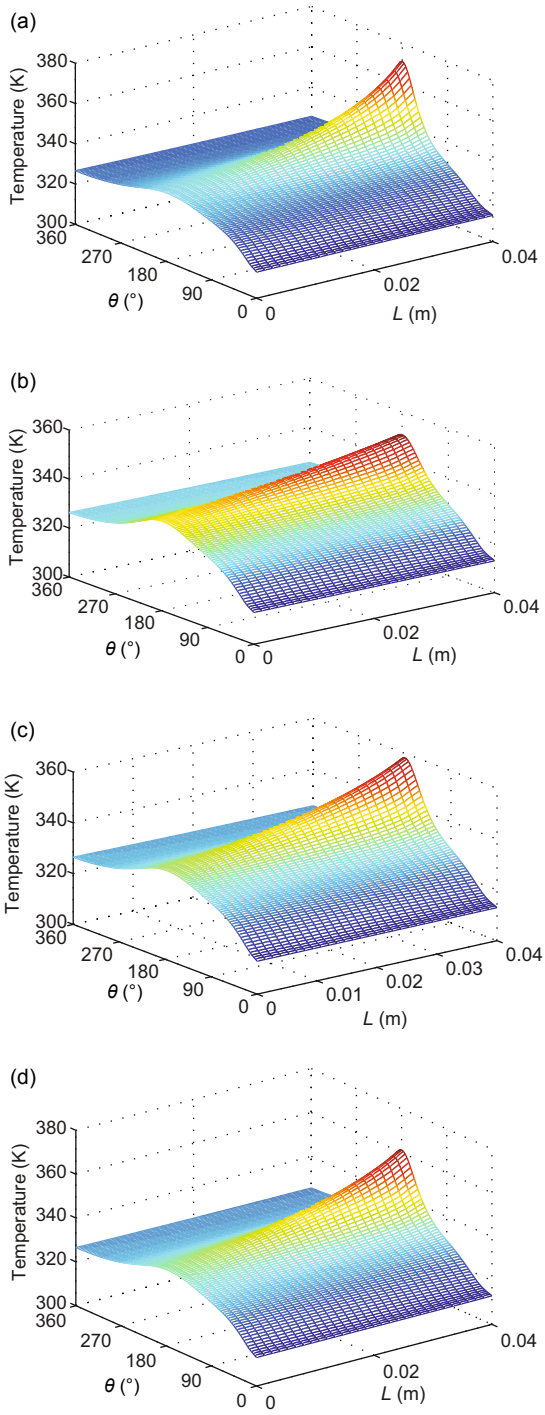

Fig. 22 Temperature field. α=0, φ=0, e=2.1×10^{-5}, L=40 mm

(a) Right bearing not considering the asymmetry deflection, d_0=0, γ=0.0210°; (b) Left bearing not considering the asymmetry deflection, d_0=0, γ=0.0112°; (c) Left bearing considering the asymmetry deflection, d_0=0, γ=0.0161°; (d) Left bearing considering the asymmetry deflection, d_0=0.03 m, γ=0.0175°

371.2 K occurs at a position of 180°. The temperature also inclines to one side like the pressure distribution. Fig. 22b shows that the maximum temperature is 350.8 K, and this time the misalignment angle is 0.0112°. Fig. 22c shows that the maximum temperature is 358.4 K, so the right bearing overestimates the temperature by 12.8 K, and the left bearing underestimates the temperature by 7.6 K. Fig. 22d shows that when d_0=30 mm, the temperature is 361.3 K. So the precise analysis model and the suitable structure parameters for the asymmetry model are very important for predicting the temperature field.

When α=π/2, φ=π/2, and d_0=0.03 m, the misalignment is 0.0175°. The oil film pressure and temperature distribution are shown in Fig. 23. This time the distribution of the oil film pressure is different from the distribution shown in Fig. 16. The maximum temperature occurs along the bearing width direction. However, another result shows that as the misalignment angle increases, the MOFP occurring at the front and rear are very clear. This time the temperature also has two peak values, one on each of these two sides.

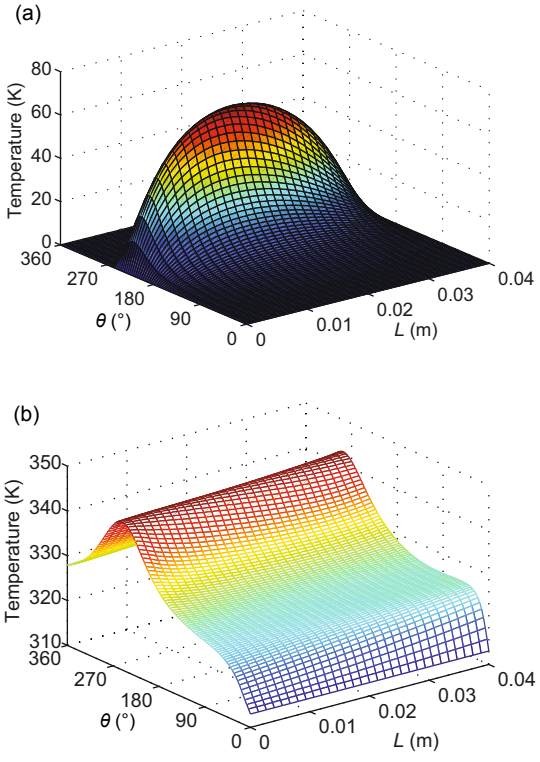

Fig. 23 Pressure (a) and temperature (b) fields

α=π/2, φ=π/2, e=2.1×10^{-5}, d_0=0.03 m, L=40 mm, γ=0.0175°

Fig. 24 shows the temperature distribution along the circumference direction when n=31. The results show that when $\alpha=\pi/2$, the peak value is different from when α=0, but the temperature along the circumference (0–70°) is higher when $\alpha=\pi/2$ than when α=0. When α=0, φ=0 and α=0, $\varphi=\pi/2$, the increase in misalignment angle can increase the temperature significantly. Comparing α=0, and φ=0 with α=0 and $\varphi=\pi/2$, the maximum temperature does not change but the point at which the maximum temperature occurs is different. The phase difference is $\pi/2$.

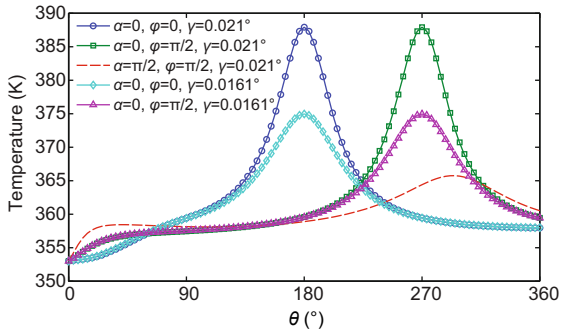

Fig. 24 Temperature distribution under different misalignments, α and φ

The oil film temperature has a strong relationship with the temperature boundary condition. The misalignment angle when the asymmetry deflection is considered is shown in Fig. 25. As the inlet temperature increases, the maximum oil film temperature increases. So controlling the inlet temperature can control the oil film temperature well.

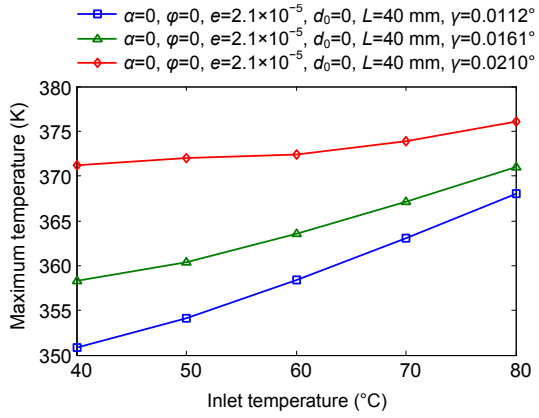

Fig. 25 Temperature changes with inlet temperature

The above analysis shows that all the structure parameters have some effect on the lubrication characteristics. A more precise model can now be established and a reasonable rotor system design can be developed that involves the rotor and the bearing. Although the genetic analysis method has little use in the step shaft in this study, it is very useful in the design. It may be particularly useful for complex rotors that consider the misalignment angle and strength to achieve a suitable value and a good match between the structure of the rotor and the bearing. This study does not consider asperity contact, which is another source of heat in the lubrication. This heat source may push the temperature higher than shown in our results (Fig. 22). If asperity contact occurs, this model needs to be corrected. Wang *et al.* (2002) found that the temperature had a strong relationship with the friction coefficient. An 8% error in the maximum temperature was observed if the friction coefficient was reduced by 10% (Zhai and Chang, 2001). The lubricant not only generated heat through viscous shearing but also played a role in cooling by transporting heat out of the thermally intensive asperity contacts. Interaction also increased the lubricant temperature away from the asperity contact. According to these papers, the heat caused by asperity has a strong relationship with the friction coefficient, so if we want to predict the temperature more precisely, the asperity model needs to be added to this model.

5 Conclusions

1. The formulation for calculating the misalignment angle of a rotor model is derived. The whole rotor system can be simplified as a step shaft problem. As well as the bending stiffness equivalent, bearing design can incorporate both lubrication analysis and structure characteristics.

2. A misalignment angle component is contributed by asymmetry deflection. The right bearing overestimates and the left bearing underestimates the oil film pressure and maximum temperature. Consideration of the asymmetry deflection has a great effect on the lubrication.

3. Leakage analysis based on the velocity was analyzed. The misalignment angle had little effect on the oil leakage, but the oil distribution was greatly influenced by misalignment, the reason that misalignment angles change the oil distribution is that it has great effect on velocity field. The maximum pressure does not occur at the same position when the misalignment angle changes and the maximum temperature of the oil film do not occur at the same point as the maximum pressure.

References

Banwait, S.S., Chandrawat, H.N., Adithan, M., 1998. Thermohydrodynamic Analysis of Misaligned Plain Journal Bearing. Proceeding of First Asia International Conference on Tribology, p.35-40.

Bouyer, J., Fillon, M., 2002. Improvement of the THD performance of a misaligned plain journal bearing. *Journal of Tribology*, **125**(2):334-342. [doi:10.1115/1.1510883]

Buckholz, R.H., Lin, J.F., 1986. The effect of journal bearing misalignment on load and cavitation for non-Newtonian lubricants. *Journal of Tribology*, **108**(4):645-654. [doi:10.1115/1.3261295]

Das, S., Guha, S.K., Chattopadhyay, A.K., 2002. On the steady-state performance of misaligned hydrodynamic journal bearings lubricated with micropolar fluids. *Tribology International*, **35**(4):201-210. [doi:10.1016/S0301-679X(01)00065-2]

Deng, M., 2008. Thermoelastohydrodynamic Analysis of Misaligned Plain Journal Bearing with Rough Surface. MS Thesis, Hefei University of Technology, China (in Chinese).

Dubois, G.B., Ocvirk, F.W., Wehe, R.L., 1957. Properties of misaligned journal bearing. *Transactions ASME*, **79**: 1205-1212.

El-Butch, A.M., Ashour, N.M., 2005. Transient analysis of misaligned elastic tilting-pad journal bearing. *Tribology International*, **38**(1):41-48. [doi:10.1016/j.triboint.2004.05.008]

Guha, S.K., 2000. Analysis of steady-state characteristic of misaligned hydrodynamic journal bearing with isotropic roughness effect. *Tribology International*, **33**(1):1-12. [doi:10.1016/S0301-679X(00)00005-0]

Gulwadi, S.D., Shrimpling, G., 2003. Journal Bearing Analysis in Engines Using Simulation Techniques. SAE Technical Paper, No. 2003-01-0245.

Jang, J.Y., Khonsari, M.M., 2010. On the behavior of misaligned journal bearings based on mass-conservative thermo-hydrodynamic analysis. *Journal of Tribology*, **132**(1):011702. [doi:10.1115/1.4000280]

Li, Q., Liu, S.L., Pan, X.H., Zheng, S.Y., 2012. A new method for studying the 3D transient flow of misaligned journal bearings in flexible rotor-bearing system. *Journal of Zhejiang University-SCIENCE A (Applied Physics & Engineering)*, **13**(4):293-310.

Liu, H.W., 1994. Mechanics of Materials. Higher Education Press, Beijing, China (in Chinese).

McKee, S.A., McKee, T.R., 1932. Pressure distribution in the oil film of journal bearings. *Transactions ASME*, **54**:149-165.

Pierre, I., Bouyer, J., Fillon, M., 2002. Thermohydrodynamic Study of Misaligned Plain Journal Bearings—Comparison Between Experimental Data and Theoretical Results. Proceedings of the Second World Tribology Congress, p.1-4.

Pierre, I., Bouyer, J., Fillon, M., 2004. Thermohydrodynamic behavior of misaligned plain journal bearings: theoretical and experimental approaches. *Tribology Transactions*, **47**(4):594-604. [doi:10.1080/05698190490513974]

Pinkus, O., Bupara, S.S., 1979. Analysis of misaligned grooved journal bearings. *ASME Journal of Lubrication Technology*, **101**(4):503-509.

Smalley, A.J., McCallion, H., 1966. The effect of journal misalignment on the performance of a journal bearing under steady running conditions. *Journal of Mechanical Engineering Science*, **181**(2):45-54. [doi:10.1243/PIME_CONF_1966_181_031_02]

Sun, J., Gui, C.L., 2004. Hydrodynamic lubrication analysis of journal bearing considering misalignment caused by shaft deformation. *Tribology International*, **37**(10): 841-848. [doi:10.1016/j.triboint.2004.05.007]

Sun, J., Gui, C.L., Li, Z.Y., 2005a. An experimental study of journal bearing lubrication effected by journal misalignment as a result of shaft deformation under load. *Journal of Tribology*, **127**(4):813-819. [doi:10.1115/1.2033007]

Sun, J., Gui, C.L., Li, Z.Y., 2005b. Influence of journal misalignment caused by shaft deformation under rotational load on performance of journal bearing. *Journal of Engineering Tribology*, **219**(3):275-283. [doi:10.1243/135065005X33937]

Sun, J., Deng, M., Fu, Y.H., Gui, C.L., 2010. Thermohydrodynamic lubrication analysis of misaligned plain journal bearing with rough surface. *Journal of Tribology*, **132**(1):011704. [doi:10.1115/1.4000515]

Timoshenko, S., Gere, J., 1972. Mechanics of Materials. Van Nostrand Reinhold, New York.

Vijayaraghavan, D., 1989. New Concept in Numerical Prediction of Cavitation in Bearing. PhD Thesis, The University of Toledo.

Wang, Y.S., Zhang, C., Wang, Q.J., Lin, C., 2002. A mixed-TEHD analysis and experiment of journal bearings under severe operating condition. *Tribology International*, **35**(6):395-407. [doi:10.1016/S0301-679X(02)00021-X]

Wen, S.Z., Huang, P., 2002. Lubrication Theory. Tsinghua University Press, Beijing, China (in Chinese).

Xu, Y.X., Li, Z.K., 1982. The Torsional Vibration of Diesel Vessel. China Communications Press, Beijing, China (in Chinese).

Zhai, X., Chang, L., 2001. Some insights into asperity temperatures in mixed-film lubrication. *Tribology International*, **34**(6):381-387. [doi:10.1016/S0301-679X(01)00027-5]

JZUS-A won the "Chinese Government Award for Publishing" for Journals

Journal of Zhejiang University-SCIENCE A (Applied Physics & Engineering) won "The Chinese Government Award for Publishing" in 2011, the highest award for publishing industry in China. It was the first time for the prize to be awarded to journals, and only 20 journals won the prize. Among them ten are science and technology journals and ten are journals of social sciences.

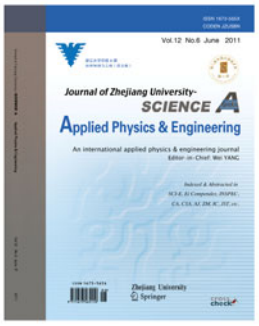

JZUS-A is an international "Applied Physics & Engineering" reviewed-Journal indexed by SCI-E, Ei Compendex, INSPEC, CA, SA, JST, AJ, ZM, CABI, ZR, CSA, etc. It mainly covers research in Applied Physics, Mechanical and Civil Engineering, Environmental Science and Energy, Materials Science and Chemical Engineering, etc.

Welcome your contribution to *JZUS-A* in the Chinese Year of the Dragon!